GSJ: Volume 10, Issue 6, June 2022, Online: ISSN 2320-9186

www.globalscientificjournal.com

SIMULATION ON PERFORMANCE OF METAL OXIDES FOR H_2S REMOVAL IN NATURAL GAS UNDER INFLUENCE OF CO_2

Jean Bosco Mutabazi[1], **Joao Chidamoio.**[2]

1.Hydrocarbon processing engineering, Chemical Engineering Department,, Eduardo Mondlane University, Maputo, Mozambique.
2. Chemical Engineering Department, Faculty of Engineering, Eduardo Mondlane University, Maputo, Mozambique
*Corresponding Author: mutaboss@gmail.com

Abstract

This research project was to simulate the performance of metal oxides for H_2S removal in natural gas under influence of CO_2. Khurmala Natural Gas Plant was chosen as a study area. To accomplish this, aspen plus version 10 was used to determine suitable metal oxides (CaO, BaO, FeO, MnO, ZnO) for desulphurization under thermodynamic equilibrium analysis, various parameters including the effect of temperature, the effect of pressure, the effect of changing CO_2, and effect of H_2S inlet were studies. The regenerability performance was monitored by considering the effect of temperature and changing pressure. The results showed reduction of H_2S in concentration reached on 0.125 ppmv for CaO (475ºC), 0.782ppmv for BaO (475ºC), 0.430 ppmv for FeO (300ºC), 0.04487 ppmv for MnO (300ºC), 0.00167 ppmv for ZnO (300ºC). Sensitivity analysis revealed that transition metal oxide is the most powerful at low performance while alkali metal oxide is the greatest at high performance. Indeed, ZnO has been shown to sustain H_2S removal capability up to 450ºC at 1atm. CO_2 has an impact on metal oxides including BaO, CaO, and MnO while metal oxides FeO and ZnO have no influence on CO_2 in the desulfurization process. The regeneration results were proven most powerful at 1atm and 400-1525ºC. Changes in temperature and pressure have a major impact on the formation of metal oxide, sulfur dioxide, and sulfate formation. It was observed that the most powerful adsorbent at a high temperatures above 300°C is ZnO> MnO> FeO>CaO> BaO, in decreasing order.

Keywords: CO_2, H_2S, natural gas, Desulphurization, metal oxides, simulation, aspen plus V10.

1. Introduction

Sulfur is contained in most hydrocarbon resources including petroleum, natural gas, and coal. Desulfurization of fuels, either before or after reforming or gasification, is important for syngas and hydrogen production and for most fuel cell applications that use conventional gaseous, liquid, or solid fuels, Sulfur in the fuel can poison the fuel processing catalysts such as reforming and water gas shift catalysts. Furthermore, even trace amounts of sulfur in the feed can poison the anode catalysts in fuel cells. Therefore, sulfur must be reduced to below 1 ppm for most fuel cells, preferably below 60 ppbv [1].

The need for a systematic risk analysis process is demonstrated by a major toxic gas disaster in the oil and gas industry. Accident reports of hydrogen sulfide emissions linked to oil and gas operations have been investigated. The storage of natural gas containing hydrogen sulfide is large and widely distributed in oil and gas processing plants [2]. The utilization of the natural gas extracted from natural resources is limited because of high corrosion environmental problems caused by acid gases [3].

Removal of sour gas impurities such as H_2S and CO_2 from gas mixtures is of vital importance for chemical industries. Natural gas usually contains H_2S, CO2 as major gas impurities. H_2S and CO_2 must be removed from natural gas before they can be used for electricity generation. Processes for separating H_2S and CO_2 include: absorption, adsorption, cryogenic and membrane techniques [4].

If present in natural gas deactivates industrial catalysts, is corrosive to metal piping, and damages the gas engines. Before it is used, transported, or sold, it must be removed from industrial operations or removed from gas. As a result, removing H_2S is critical for the preservation of pipeline systems and catalysts in chemical processes [5].

The most known method for H_2S separation is amine scrubbing. Although high product yields and purities can be achieved, this process has the disadvantage of high energy consumption along with substantial liquid losses due to solvent evaporation in the stripper,[6].

Adsorption systems are typically suitable for low gas flow rates and low H2S concentrations. Among the available adsorbents, metal oxides are contemplated to be a valuable choice for H_2S elimination,[7]. Numerous methods for the removal of H_2S have been developed but little has been reported on the use of metal oxides [8].

However CO_2 concentrations in natural gas can affect the H_2S retention concentration with adsorbent. Many authors stated the presence of CO_2 in feed gas decreased the H_2S removal or doesn't have any effect according to the operation condition or type of adsorbent used [9],[10].

The main motivation for this project is to extend other adsorbents such as metal oxides to include processes required for the deep purification of NG, more precisely for its sweetening. Thus, the focus of this work is the modeling and simulation of desulfurization processes using the aspen plus version 10 software, applying the tools available in the simulator database to satisfactorily reproduce desulfurization operation behavior. Sensitivity analysis will be performed to observe the influence of significant parameters affecting the process (pressure and temperature) on the properties of the synthesis gas produced the specification.

2. Methods

2.1. Feed natural gas composition

Simulation and Optimization used by amine: a Case study of Khurmala Field in Iraqi Kurdistan Region January, 2014 [11]**.**

Table 1.*Natural gas composition*

Component	%	Molar flowrate	Mass flowrate
Methane	0.716414328	3840.634661	61614.91813
Ethane	0.15650313	838.9996154	25228.63496
Propane	0.060601212	324.8778063	14326.13667
i.butane	0.015300306	82.02360457	4767.540037
n-butane	0.027600552	147.9641494	8600.268302
i-pentane	0.011400228	61.11562693	4409.553659
n-pentane	0.008300166	44.49646522	3210.464506
n-hexane	0.001300026	6.969325878	600.6018841
H_2S	4.00E-05	0.214440796	7.308334965
H_2O	0.002300046	12.33034578	222.1324183
CO_2	4.00E-05	0.214440796	9.437475277
Nitrogen	0.000200004	1.072203981	30.03565065
Flowrate	100	5360.912686kmol/h	123027.032025785kg/h
Temperature	40 ^{O}C		
Pressure	3555kpa		
Volume flowrate	3776 m^3/h		

2.2. Metal Component Used in Desulfurization and regeneration

The components used in the desulphurization, and regeneration simulations are listed as: Calcium, Barium, iron, manganese and Zinc based oxides are the most extensively studied oxides for desulfurization in

solid−gas reactions due to their high affinity to sulfur.

Table 2.metal components considered in the desulphurization simulations.

Metal	**Feed sorbent**	**Component in simulation**
Ca	CaO	Ca, CaO, $CaCO_3$, CaS
Mn	MnO	Mn, MnO, Mn_3O_4,Mn_2O_3, MnO_2, MnS, MnS_2,Mn_3C, $MnCO_3$
Zn	ZnO	Zn, ZnO, ZnS,$ZnCO_3$
Ba	BaO	Ba, BaO, $BaCO_3$, BaS
Fe	FeO	Fe, FeO, Fe_2O_3,Fe_3O_4, FeS, FeS_2,Fe_3C, $FeCO_3$,C

Table 3. Components considered in the regeneration simulations Phase

Phase	**Component**
Gas	O_2,N_2,SO_2,CO_2
Solid	CaS,$CaCO_3$,$CaSO_4$,ZnO,ZnS, $ZnSO_4$,MnO,MnS, $MnSO_4$,BaO,,$BaCO_3$,BaS, FeO,FeS,$FeSO_4$

2.3. Modelling Aspen in desulphurization process

The Aspen Plus flow-sheet for the natural gas desulfurization is shown in figure 1 The development of a model in Aspen Plus involves the following steps**:** Specification of the stream class, selection of the property method, specification of system components (from a data bank), identifying conventional and solid component, defining the process flow-sheet. The feed streams (flow rate, composition, and thermodynamic state), as well as unit operation blocks (thermodynamic condition, chemical reactions, and so on) are then provided.

2.4. Process Assumptions made

In developing the equilibrium models in Aspen Plus, the following assumptions were taken into account:
- The process happens under steady-state circumstances.
-All reactions approach equilibrium, and kinetics are not taken into account.
-Inside the reactors, the pressure and temperature remain constant.
-The gases involved obey the ideal gas law [12].
-All C1, C2, C3, iC4, n-C4, i-C5, n-C5, and n-C6 are inert

2.5. Description of Aspen Plus flow-sheet

Desulfurization units typically come with two towers, A and B. In practice, tower A is operational and removes H_2S, whilst tower B is inactive or undergoing regeneration.

The feed of natural gas composition was specified as convention stream and the molar flowrate of 5360.9kmol/h with 35.5bar and 40 ^{O}C. The gas stream pass to the heater1 block where gas is heated at 100 ^{O}C to avoid below dew point. The outlet stream goes to the expender block where the gas is expended at 1atm, because when expending its temperature decreases the streams is entering in the second heater block Heat2 where the temperature increases at 300 ^{O}C, other hand the stream of Metal-oxide with 0.2358851kmol/h, 1atm and 300 ^{O}C specified as CIPSD entering in defined Adsorbent reactor specified as the RGIBBS Block. The gas stream reaches the Metal oxide in RGIBBS where the reaction of desulfurization and other chemical reaction occurs.

The natural gas composition was changed using a constrained equilibrium model in the RGIBBS block with the use of a temperature approach for the reactions, which were set at temperatures and pressures ranging from 300^{O}C to 525^{O}C and 1 atm, respectively, depending on the adsorbent type.

The process flowsheet of desulfurization and regeneration is shown in the figure below

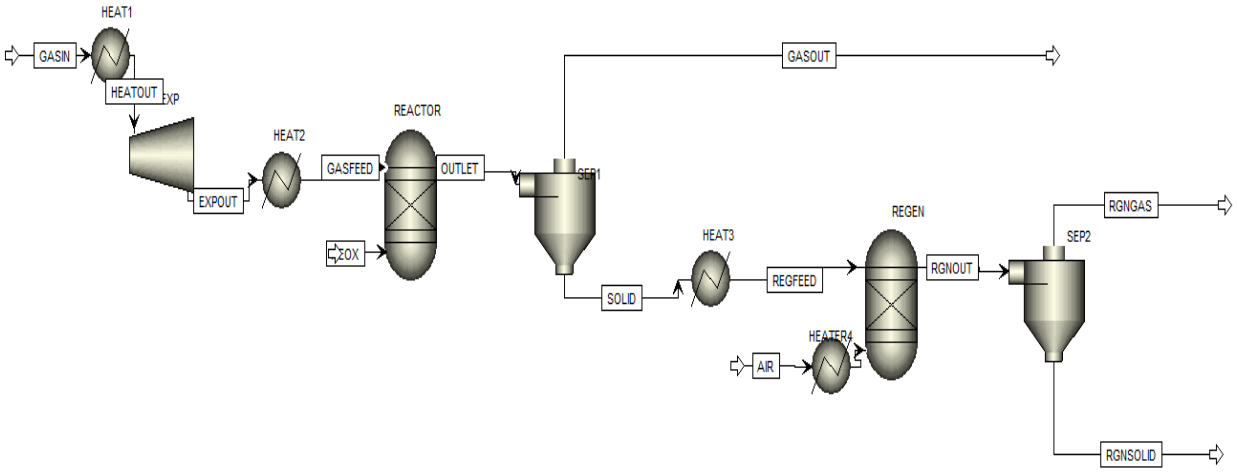

Figure 1. The process flowsheet of desulfurization and regeneration.

This empirical approach was proposed by González-Vázquez [13] where the gas composition can be adjusted to match the experimental data obtained in the pilot plant using the Aspen tool "Data Fit" to modify reaction equilibrium, . To apply this approach, the reactions involved in the system should be independent, the natural gas from C1, C2, C3, iC4, n-C4, i-C5, n-C5, n-C6, and N_2 were set as inert in this reactor.

The outlet component mixture which contained metal sulfide, metal carbonate were separated and the solid outlet passed to the HEATER block are sent to the second RGIBBS Block where chemical equilibrium takes place specified as regenerator where it reach Air stream contained Convention O_2/N_2 where the oxidation of metal sulfide into metal oxide and unwanted reaction are maintained. The regenerator was set at temperature and pressure of 500 ^{O}C to 1750 ^{O}C and 1atm respectively according to the metal sulfide type. After regeneration of metal oxide gas components are recycled to the adsorbent reactor it reaches other gases. All metal oxides were taken as 10% of excess to ensure all reactant were consumed.

Similarly, cyclones at the outlet of each reactor CYCLONE1 and CYCLONE2 are used to separate the solid and gaseous products resulting from both reactors. For the case of the first separation the resulting solids (Zinc, Manganese, Barium, calcium and iron and tungsten) are disposed of reagents for the second reactor and the separated gas (GAS-1) constitutes sweet gas. In the second reactor, according to reactions (3) and (5) the solid products, which are separated by the second cyclone comprise regenerated oxides.

Table 4. Reactor block description used in the simulation

Block ID	**Aspen Plus name**	**Description**
Heater 1	Heater	Preheat natural gas to 100^{o}C
Heater 2	Heater	Heat expended gas outlet to 300^{o}C
Heater 3	Heater	Heat react outlet metal sulfide to different temperatures accordingly
Expender	Heater	Expend gas from 35.5 bar to 1atm
Reactor	RGIBBS	Equilibrium reactor; models single -Phase chemical equilibrium or simultaneous phase and chemical equilibrium by minimizing Gibbs free energy. -It useful when temperature and pressure are known and reaction stoichiometry is unknown
RGNR	RGIBBS	-Equilibrium reactor; models single phase chemical equilibrium or simultaneous -Phase and chemical equilibrium by minimizing Gibbs free energy.

		-It useful when temperature and pressure are known and reaction stoichiometry is unknown
Separator 1	Cyclone	Separate reactor outlet gas and solid
Separator 2	Cyclone	Separate regenerator outlet metal oxide and gas

2.6. Gibbs Reactor Modelling

When static chemical balance is achieved, Gibbs reactor is a virtual device that is used to compute the components ratio and related features of the mixture. The Gibbs Reactor simulates a chemical reactor by solving the heat and material balances based on minimizing the free energy of the components in the reaction,[14]. The Gibbs reactor determines the component distribution that is predicted when the system is in chemical equilibrium. Reaction stoichiometry may be defined in the Reaction Data Sets window and used in the Gibbs reactor [15].Gibbs reactor in Aspen Plus does not require specified reaction stoichiometry [16].

In this work, the C1, C2, C3, iC4, n-C4, i-C5, n-C5, and n-C6 are set as inert, the calculation determines the distribution of the components, which gives the minimum free energy for the system. Reaction stoichiometry may be defined in the Reaction Data Sets window and used in the Gibbs reactor. The temperature and pressure were specified due the type of sorbent.

2.7. Desulfurization reaction

The desulfurization reactor involves thermodynamic equilibrium as stated the reaction Equation has a high equilibrium constant which means the forward reaction is favorable as stated in the reaction below:

$$MeO_{(s)} + H_2S_{(g)} \leftrightarrow MeS_{(s)} + H_2O_{(g)} \quad (1)$$

(1), The equilibrium constant for reaction has defined in the equation (2)

$$K_p = \frac{[H_2O]}{[H_2S]} \quad (2)$$

Obeys the thermodynamic relation

$$K_p = \exp(-\frac{\Delta G}{RT}) \quad (3)$$

T is the temperature, and R is the gas constant, and DG is the standard Gibbs free energy change of reaction (Equation (1)).

The reaction below indicates sulfurization of different metal oxides and removal of carbon dioxide with the corresponding enthalpy of reaction.

$CaO_{(s)} + H_2S_{(g)} \leftrightarrow CaS_{(s)} + H_2O_{(g)}$	$\Delta H_{298k} = -104 Kj/mol$ (4)
$CaO_{(s)} + CO_{2(g)} \leftrightarrow CaCO_{3(s)}$	$\Delta H_{298K} = -178.5 Kj/mol$ (5)
$FeO_{(s)} + H_2S_{(g)} \leftrightarrow FeS_{(s)} + H_2O_{(g)}$	$\Delta H_{298K} = -93.78 Kj/mol$ (6)
$FeO_{(s)} + CO_{2(g)} \leftrightarrow FeCO_{3(s)}$	$\Delta H_{298K} = -11.64 Kj/mo$ (7)
$BaO_{(s)} + H_2S_{(g)} \leftrightarrow BaS_{(s)} + H_2O_{(g)}$	$\Delta H_{298K} = -147.41\, Kj/mol$ (8)
$BaO_{(s)} + CO_{2(g)} \leftrightarrow BaCO_{3(s)}$	$\Delta H_{298K} = -238\, Kj/mol$ (9)
$MnO_{(s)} + H_2S_{(g)} \leftrightarrow MnS_{(s)} + H_2O_{(g)}$	$\Delta H_{298K} = -95.02\ Kj/mol$ (10)
$MnO_{(s)} + CO_{2(g)} \leftrightarrow MnCO_{3(s)}$	$\Delta H_{298K} = -32.9\, kj/mol$ (11)
$ZnO_{(s)} + H_2S_{(g)} \leftrightarrow ZnS_{(s)} + H_2O_{(s)}$	$\Delta H_{298K} = -119.92\, kj/mol$ (12)
$ZnO_{(s)} + CO_{2(g)} \leftrightarrow ZnCO_{3(s)}$	$\Delta H_{298K} = -73\, kj/mol$ (13)

The enthalpies of production of the reactants and products were used to calculate the values in the Equations above[16]. Notice that the reaction of sulfurization and carbon dioxide removal with metal oxide

is exothermic. As a result, as the temperature rises, the equilibrium constant lowers, making the equilibrium less favorable for the metal sulfide [17].

3.8. Regeneration reaction

Regeneration involves chemically converting the metal sulfide formed during sulfurization, back to the oxide form, typically by subjecting it to oxidation, either in air, oxygen, or steam, at temperatures that are a couple of hundred degrees higher than the sulfurization temperature [18].

$$MeS_{(s)} + {}^{3}/_{2}\ O_{2(g)} \leftrightarrow MeO_{(s)} + SO_{2\,(g)} \quad (14)$$

$$K_p = \frac{P^{-1/2}X[SO_2]}{[O_2]^{3/2}} \quad (15)$$

An unwanted side-reaction is the formation of sulphates:

$$MeS_{(s)} + 2O_{2(g)} \leftrightarrow MeSO_{4(s)} \quad (16)$$

$$K_p = P^{-2}X[O_2]^{-2} \quad (17)$$

The regeneration reactions and their corresponding enthalpy of reactions are represented below

$CaS_{(s)} + \frac{3}{2}O_{2(g)} \leftrightarrow CaO_{(s)} + SO_{2(g)}$	$\Delta H_{298K} = -458.62\,Kj/mol$ (18)
$CaS_{(s)} + 2O_{2(g)} \leftrightarrow CaSO_{4(s)}$	$\Delta H_{298K} = -960.9\,Kj/mol$ (19)
$BaS_{(s)} + \frac{3}{2}O_{2(g)} \leftrightarrow BaO_{(s)} + SO_{2(g)}$	$\Delta H_{298K} = -415.24\ kj/mol$ (20)
$BaS_{(s)} + 2O_{2(g)} \leftrightarrow BaSO_{4(s)}$	$\Delta H_{298K} = -1001.61\,kj/mol$ (21)
$FeS_{(s)} + \frac{3}{2}O_{2(g)} \leftrightarrow FeO_{(s)} + SO_{2(g)}$	$\Delta H_{298K} = -468.87\,Kj/mol$ (22)
$FeS_{(s)} + 2O_{2(g)} \leftrightarrow FeSO_{4(s)}$	$\Delta H_{298K} = -832.2\,kj/mol$ (23)
$MnS_{(s)} + \frac{3}{2}O_{2(g)} \leftrightarrow MnO_{(s)} + SO_{2(g)}$	$\Delta H_{298K} = -467.63\,kj/mol$ (24)
$MnS_{(s)} + 2O_{2(g)} \leftrightarrow MnSO_{4(s)}$	$\Delta H_{298K} = -852.5\,Kj/mol$ (25)
$ZnS_{(s)} + \frac{3}{2}O_{2(g)} \leftrightarrow ZnO_{(s)} + SO_{2(g)}$	$\Delta H_{298K} = -442.7\,Kj/mol$ (26)
$ZnS_{(s)} + 2O_{2(g)} \leftrightarrow ZnSO_{4(s)}$	$\Delta H_{298K} = -775\,Kj/mol$ (27)

3. RESULT AND DISCUSSION

3.1. Reactor Operating Condition and Specification

The aspen plus version 10 specification parameters with operating conditions are used to simulate desulphurization with metal oxide. 5 metal oxides with 5 cases of aspen flowsheet were tested using thermodynamic criteria for desulfurization capabilities at temperature ranges of (25-600 OC) and (1-20atm).

The reactor shows that it works under phase equilibrium and chemical equilibrium, this implies the minimization of Gibbs free energy, the pressure, and temperature and inert compounds are specified accordingly

3.2. Sensitivity Analysis

A sensitivity analysis was undertaken to assess the impact of changes in process parameters and/or configuration on net efficiency. As a result, the sensitivity analysis gives an idea of the influence on efficiency at various capture rates,[19].

This work has six sensitivity analyses were performed to determine optimal operating process conditions. The first four operate in first reactor of sulfur retention including temperature and pressure change, the impact of CO_2 inlet and inlet H_2S on the H_2S outlet. The Fifth and sixth one is sensitivity analyses will be

carried out in the second reactor and analyses the variation of the operating temperature and pressure at which regeneration of Metal oxides is expected to occur.

3.3. Desulfurization Result with Different Metal Oxides

Simulation data of H_2S concentrations at various reaction were obtained by reacting H_2S with metal oxide and CO_2 with metal oxides formulated at our aspen plus version 10. Several simulation runs were made to evaluate the adsorption of H_2S into the Gibbs reactor at various temperatures.

3.4. Effect of Temperature Inlet on desulphurization

The simulation was conducted at different temperatures to determine the optimum temperature providing the highest adsorption performance of H_2S removal and influence on CO_2. Inlet H_2S concentration as low as 41ppmv was selected to simulate a natural gas stock with average sulfur content and the inlet concentration of CO_2 selected in the feed natural gas Temperature has set at 25 ^{O}C and above.

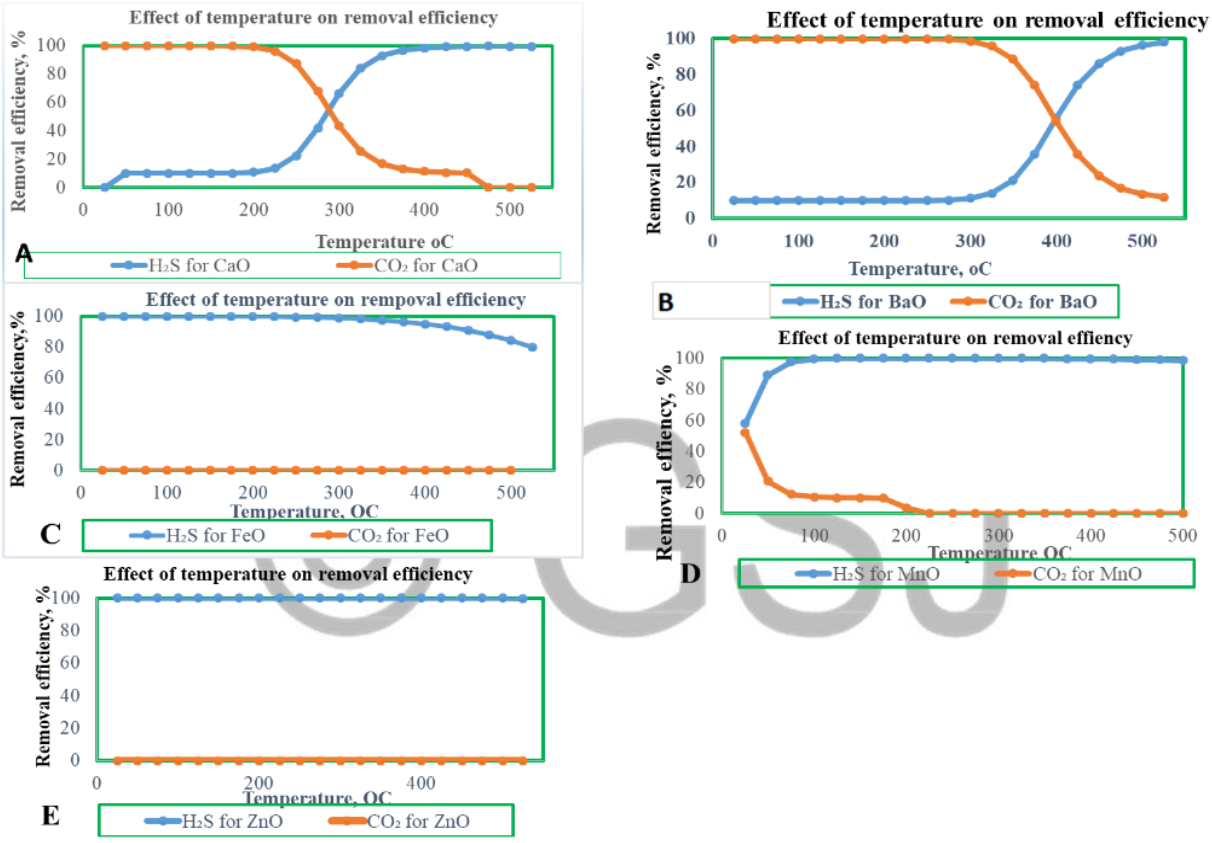

Figure 2. Effect of temperature on desulfurization

Figure 2 shows the effect of reaction temperature on H_2S outlet and CO_2 outlet concentration of various adsorbents including BaO, CaO, FeO, MnO, and ZnO. H_2S outlet concentration for all sorbents used is defined as the amount of H_2S that remaining after adsorption and the amount of CO_2 adsorbed at the sorbent's surface related to the H_2S concentration at the outlet and CO_2 concentration respectively.

Figure 2 (C) and (E) above show that an increase in the reaction temperature from 25 ^{O}C to 300 ^{O}C decreased H_2S removal efficiency at the reactor outlet for adsorbent FeO, and ZnO. In numbers, the removal efficiency decreased from 99.99% to 99.8% for ZnO, and 99.99% to 84.1% for the FeO, although ZnO showed a good performance at low temperature until 425 ^{O}C where H_2S outlet concentration remained 17ppbv. The influence of CO_2 on FeO and ZnO shows no significate effect. These results have a good agreement with Neveux, 2013 who reviewed ZnO sorbent shows high efficiency which is can maintained 99.9% with great potential in reducing H_2S concentration to below 20ppbv at below 450 ^{O}C,[7] The results also show the removal efficiency of H_2S on MnO in figure 9 (D) increased from 57.84% at 25 ^{O}C to 99.98 % at 200 ^{O}C and starts to decrease as the temperature increase. At 300 ^{O}C the removal efficiency of 99.89% with an outlet concentration of 0.0449ppmv to 98.3% at 500 ^{O}C with an outlet concentration of 0.692ppmv while the CO_2 removal efficiency was found to decrease from 52.15% at 25 ^{O}C to 0.0003% at 500 ^{O}C, it is shown that at 200 ^{O}C most of CO_2 removed. it is shown that MnO good

performance was kept until 350 ^{O}C, with removal efficiency of 97.5% and 0.99ppmv in term of concentration however it was found the obtained results are is in line with the literature [20] who study the effect of the temperature on H_2S removal under CO_2, he stated that at medium temperature MnO is the stable form.

From a thermodynamic point of view, manganese is a most promising sorbent, The positive correlation between CO_2 saturation loading and temperature was not clarified by the authors[23] Kumar et al. 2014 conducted lower temperatures (25, and 200 ^{O}C) resulted in reduced saturation loadings for CO_2, the driving force for MnO to convert in $MnCO_3$ was high even at a low temperature 77 ^{O}C at 1atm. and conclude that as the temperature increases, the adsorption of CO_2 decreases but as the gas-phase partial pressure of CO_2 increases, CO_2 adsorption increases accordingly,[7].

Figure 2(A) and (B) also show a low removal efficiency for H_2S at low temperature for BaO and CaO and favor the CO_2 removal. Figure.2 (A) shows the removal efficiency of H_2S by CaO increases from 25 OC of 0.0% to 475 ^{O}C of 99.6% and decreases from 475 ^{O}C to 525 ^{O}C of 99.6% to 99.4% respectively. It indicates the concentration of 41ppm to 0.15ppmv and 0.150ppmv to .0.246ppmv respectively. For BaO adsorbent it shows the increase of removal efficiency from 25 ^{O}C to 525 ^{O}C, in number from 10% to 98% with outlet concentration 37ppm to 0.8ppm. Besides that figure 9(A) and (B) show CO_2 removal efficiency decrease from 25 ^{O}C to 525 ^{O}C, in number from 99.99% to 0.001% for CaO adsorbent and 100% to 11% for BaO adsorbent.

However, it is stated that CaO and BaO were absorbents of hydrogen sulfides in the temperature range of when the reaction temperature is increased to high temperatures leads to calcium oxides and Barium oxide start to make a greater contribution to H_2S removal. This may be attributed to competitive adsorption between H_2S and CO_2.which resulted from H_2S and CO_2 coadsorption, CO_2 being either present as traces in H_2S, [21].

The result obtained also are in the line of Carnes et al. 2002, who investigated the adsorption of H2S on microcrystalline metal oxides of Zn, Ca, Mg, and Al at high (250 -500 ^{O}C) and low temperatures (25-100 ^{O}C) and they concluded that at elevated temperatures, CaO was the best choice for H_2S adsorption.

Generally, many authors came to the conclusion that the smaller the band gap in the oxide, the higher the reactivity of the system over S–containing species. Oxides with high ionic character, such as BaO and CaO, exhibited low reactivity with H_2S and High reactivity of CO_2, illustrating that the electrostatic interactions taking place between the dipole of H_2S and the ionic field being generated by the charges in an oxide were of subordinate importance in the adsorption process. On the other hand, FeO, ZnO and MnO have low ionic character interacted strongly with H_2S, and less by CO_2 As a result, it was discovered that the lower the band gap energy, the greater the amount of H2S adsorbed,[22].

3.5. Effect of Pressure Inlet

The pressure was varied from 1 to 20atm, the figure below shows the effect of the pressure reactor at different temperature kept constant, depending on the sorbent ranging from 300 to 525 ^{O}C.

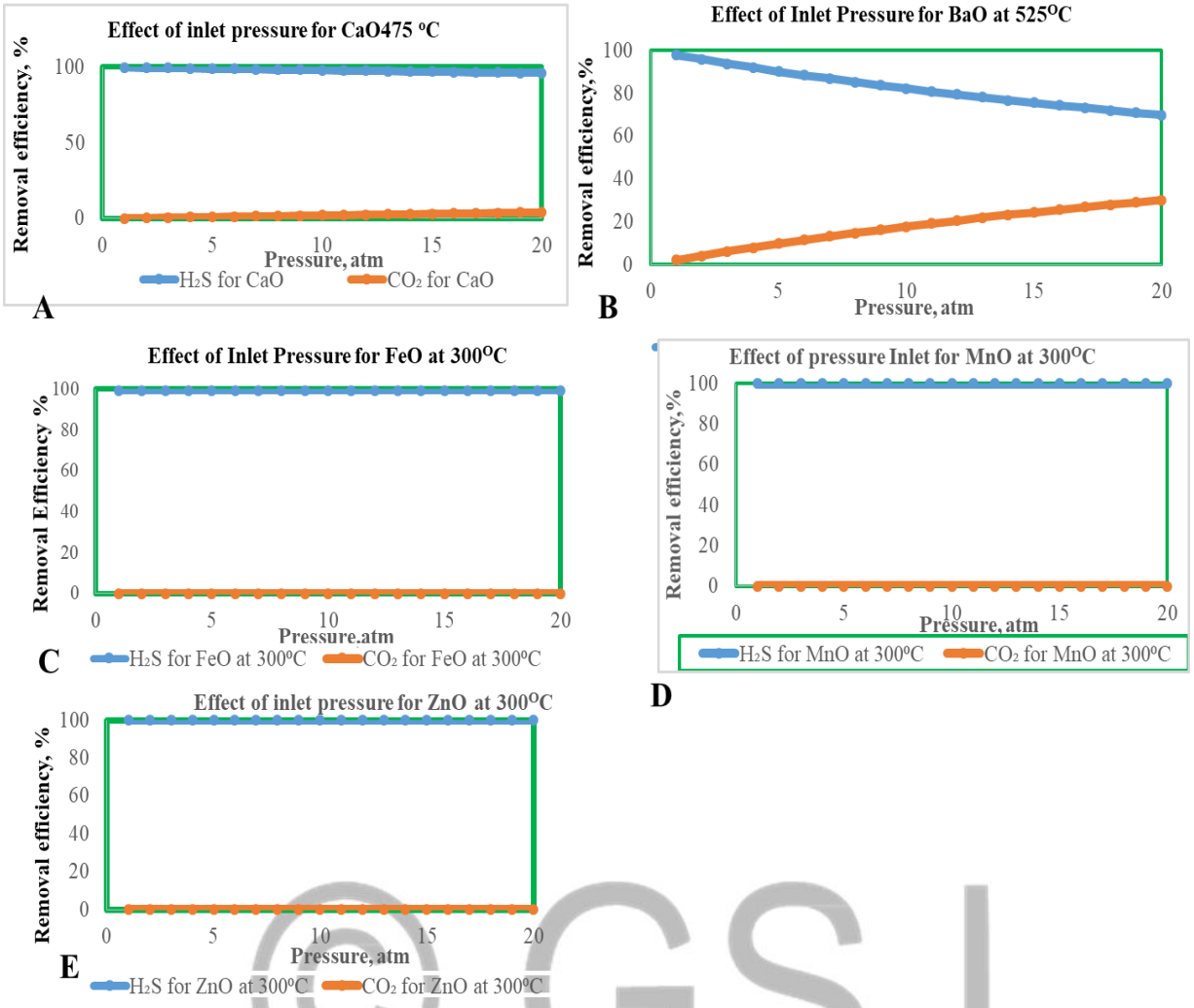

Figure 3. Effect of changing pressure in desulfurization

As shown that Figures 3 (A) and (B), when increasing the pressure inlet of the reactor from 1atm to 20atm, the removal efficiency of H_2S decreases while CO_2 removal efficiency increases. In number CaO at 475^{O}C, H_2S removal efficiency decreases from 99.6% to 95.9% related to concentration of 0.150ppmv to 2ppmv respectively. While for CO_2 removal efficiency increased from 0.00015% to 4%. Regarding BaO, figure 3(B) show the H_2S removal efficiency decreased from 97.8% to 69.88% corresponding of 0.8ppm to 1.12ppm respectively, while CO_2 increased from 2.12% to 30%. This decrease in the sulfurization rate with increasing pressure was explained based on of a decrease in the mass transfer coefficient and effective diffusivity with increasing pressure [23], this may be due to the l*e chatelier* principle where the increase in pressure favouring the equation of the removal of CO_2 while the equation of H_2S removal remains constant. See equations (1), and (8)

For, FeO, MnO and ZnO adsorbents it was shown that the increase of pressure doesn't have any significate effect on CO_2 and H_2S removal efficiency. This result shows a similar trend to a previous study by Wang, where in the total pressure change in the gas phase does not affect the breakthrough curve characteristics when the other operating conditions are kept constant,[24].

3.6. Effect of H_2S Inlet

When comparing the model gases that contain different H_2S concentrations, a reduction in the alkali specificity was observed. The alkali specificity value decreased as the H_2S content increased. Regardless of the H_2S content in the model gases, the removal efficiency remained consistent, indicating that the alkali absorption method is more efficient in terms of selective H_2S removal, [27][25].

The Effect of inlet H_2S concentration Figure 4 shows the effect on H_2S outlet concentration for natural gas with inlet 0.05361kmol/h, 0.10722kmol/h, and 0.214441 of H_2S flowrate at 1atm and temperature range of 300-525 ^{O}C accordingly.

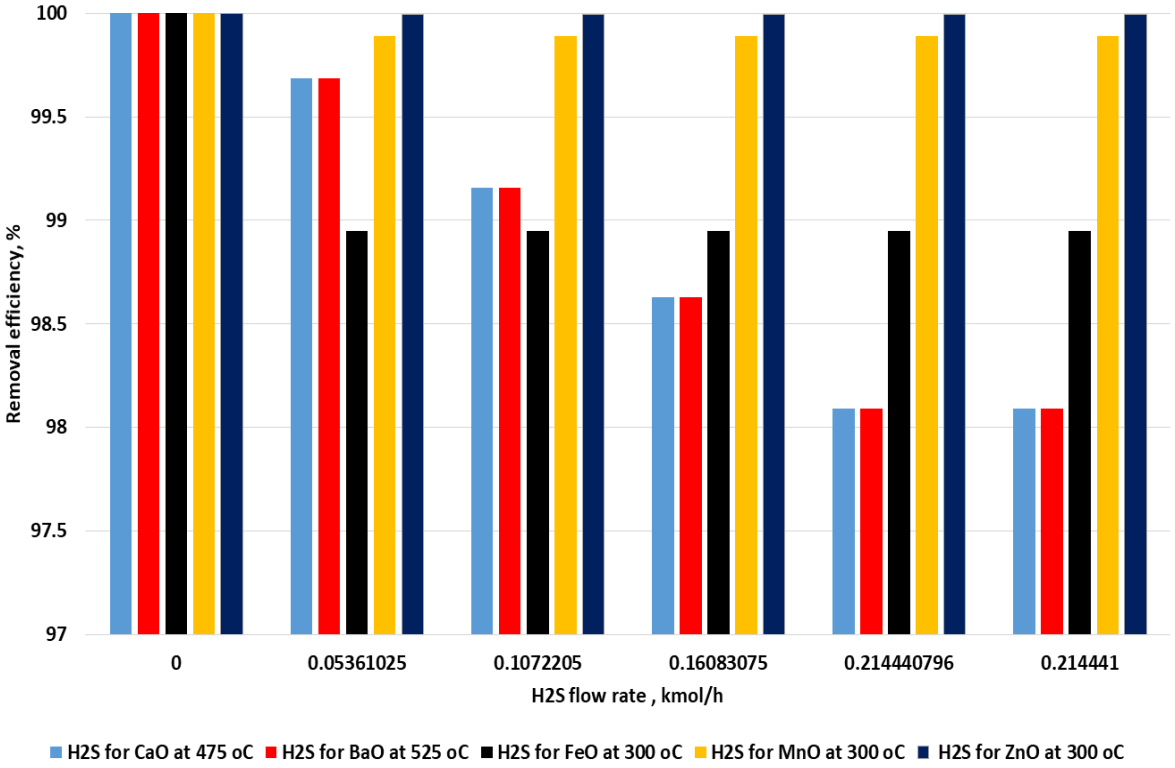

Figure 4. Effect changing H_2S Inlet in desulfurization

It is observed that by increasing H_2S inlet concentration, the removal efficiency decrease for BaO and CaO adsorbent. The alkali absorbent shows little sensitivity to the changes in the H_2S content of the inlet gas, [25]. In numbers for CaO at 475 ^{O}C, the removal efficiency of H2S decrease from 99.68% to 98.08% corresponding to 150ppbv to 0.82ppmv respectively.
Other transition sorbents including FeO, MnO and ZnO show no significant change when changing from 0.05261kmol/h, 0.10722, 0.1608kmol/h. This is in line with the results observed by obek, 2016. Showing that the efficiency of H_2S removal does not depend on the H_2S concentration in this process [25].

3.7. Effect of CO_2 Inlet

Effect of inlet H_2S concentration Figures 8 to 10 show the effect on H_2S outlet concentration for natural gases with 0.05361 kmol/h, 0.10722kmol/h, and 0.214441kmol/h of CO_2 inlet concentration

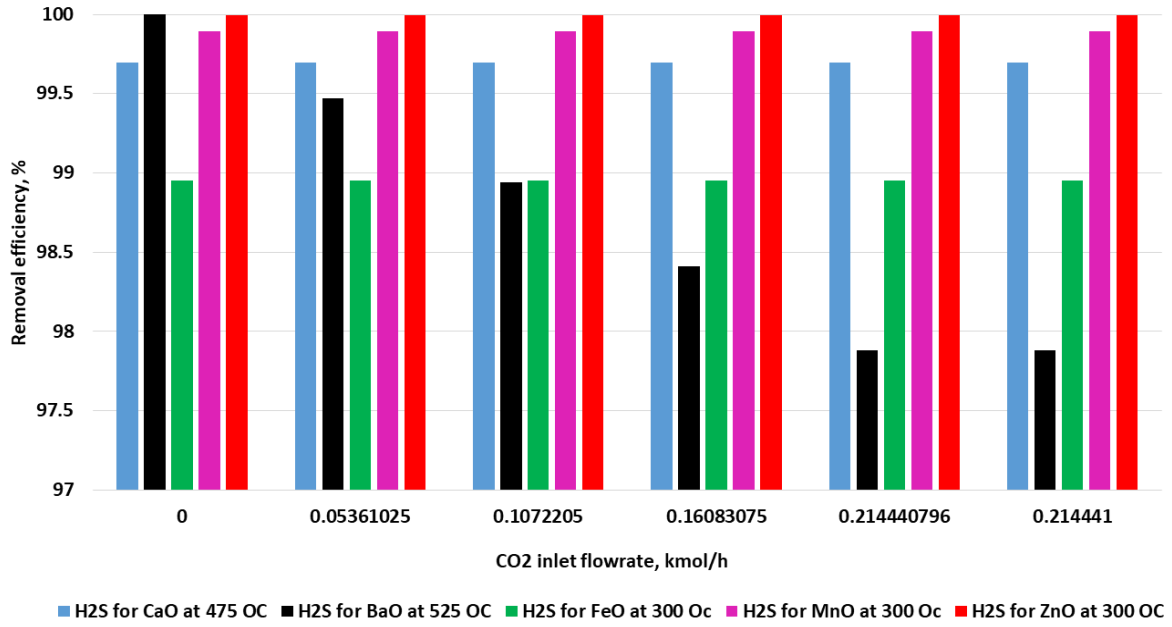

Figure 5. Effect of CO_2 inlet in desulfurization

It was shown that as increasing CO_2 inlet concentration does not affect on sorbent including, CaO at 475 ^{O}C, FeO at 300 ^{O}C, MnO at 300 ^{O}C, and ZnO at 300 ^{O}C. The outlet H_2S concentrations in all the tests broke at almost the same time. Hong et all,2008 suggest that water, CO and CO_2 had no significant effects on the breakthrough time and desulfurization performance at room temperature up to 475 ^{O}C at 1 atm [26]. But it has an effect on BaO at 525 ^{O}C, decreasing the removal of H_2S efficiency as increasing CO_2 inlet concentration, in values, it decreases from 99.99% to 97.88% corresponding to 5ppb outlet concentration to 0.92ppm outlet concentration. This was concluded by Novochinskii, 2004 that the thermodynamic equilibrium is slightly worse in case CO_2 is present. It was also reported that the inhibitory effect (CO_2 inhibits the adsorption of H_2S) was higher for BaO which show shows that the efficiency of H_2S removal is decreased by increasing CO_2 content. It can be concluded that introducing CO_2 into the feed gas affected the H_2S adsorption capacity of the sorbent [27].

Despite the fact that CO_2 is a stronger acid than H_2S, it is a slower adsorber, hence H_2S can be absorbed in a short period of time. It was shown that shows that the efficiency of H_2S removal is decreased by increasing CO_2 content. The competition between H_2S and CO_2 in alkali absorbents [24].

3.8. Regeneration of metal oxide

Regeneration of the sulfided metals were performed by direct oxidation with air to form the metal oxide with the conversion of the sulfur as sulfur dioxide and metal as metal oxide,[28].

The regeneration was made with 5 metal oxides, the Gibbs reactor as the regenerator of optimum temperature reactor of different metal oxide and 1 atm.

3.8.1. Effect of Temperature on Regeneration of metal oxide

As Thermodynamic calculations are often used as a first indication of the feasibility of a suggested regenerative process. The influence of temperature in the range of 300−1600 ^{O}C is also shown in Figures representing various sorbent BaO, CaO, FeO, MnO, and ZnO. The findings demonstrate that a higher temperature is beneficial to regeneration [33],[29].

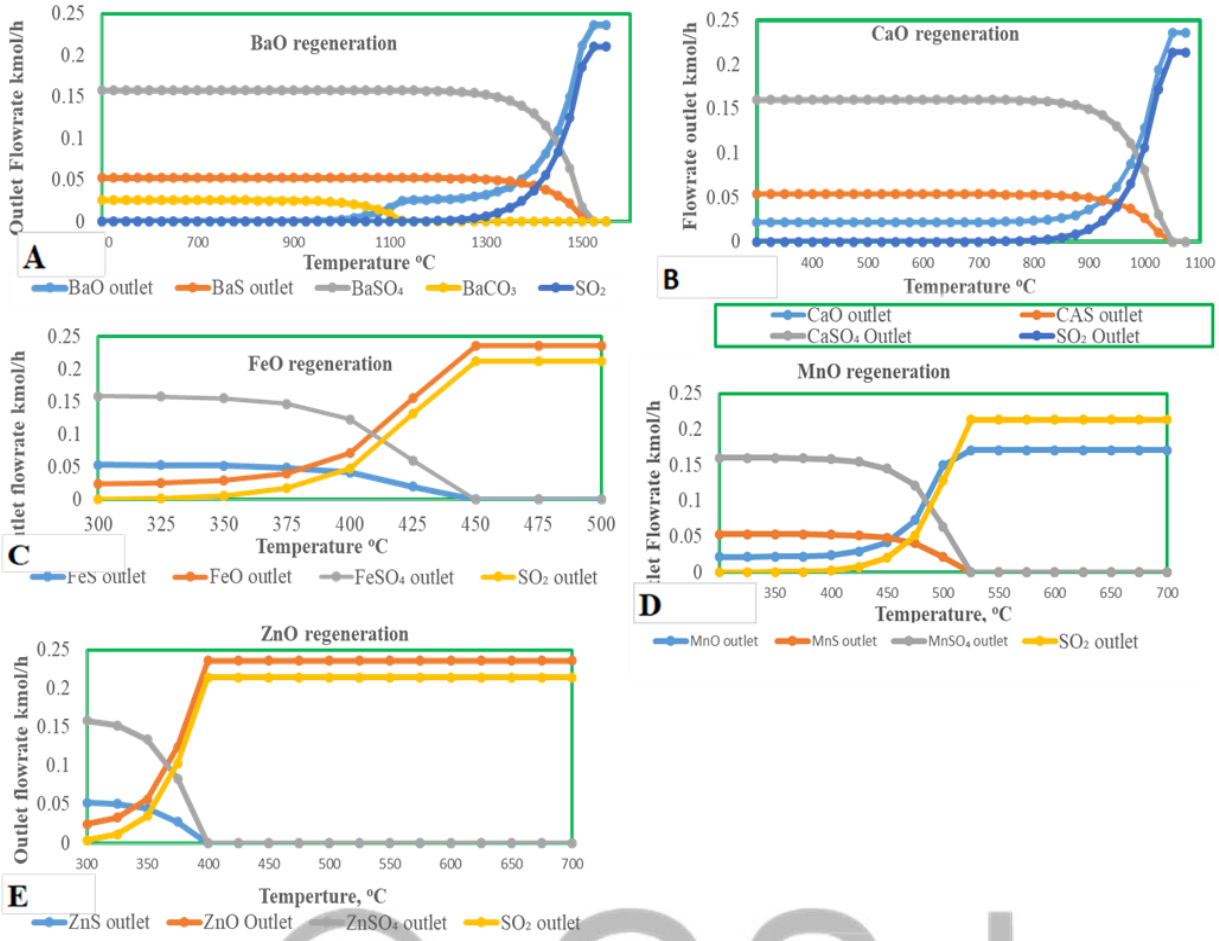

Figure 6.Effect of temperature on regeneration

Figure 6 shows the increase in temperature leads to the increase in regeneration of sorbent, it is shown that the regeneration of CaO, Figure 13(A) increases from $1.31*10^{-12}$kmol/h at 350 ^{O}C to 0.213787kmol/h at 1050 ^{O}C, in other hand $CaSO_4$ formed in 0.16034kmol/h at 400 ^{O}C to 0.0311077kmol/h at 1025 ^{O}C, it can be seen that below 1050 ^{O}C at 1atm the sulfate formation is favored, to overcome that challenge, it advisable to run at temperature above 1050 ^{O}C.

For BaO, figure 6(B) increase from $4.07*10^{-12}$kmol/h at 650 ^{O}C to 0.21048kmol/h at 1525 ^{O}C. Below the above a temperature favors the formation of sulfate which where decreased from 0.157764kmol/h at 300 ^{O}C up to 0.018011kmol/h at 1500 ^{O}C, it is observed that to prevent the formation of $BaSO_4$, the BaO set at 1525 ^{O}C at 1atm.

It is indicated that CaO and BaO are very resistant to reduction. However, as mentioned before, due to the stability of its sulfate, it has been examined as a non-regenerable sorbent. In such an application, the bed material should be stabilized to $CaS0_4$ form, which is more suitable for disposal in landfills. However, problems exist with both the overall reaction rate of sulfidation which is limited by pore and product layer diffusion, and with stabilization of CaS to $CaS0_4$, [34][30].

The regeneration of FeO, figure 6(C)) increase from 0.00043kmol/h at 300 ^{O}C to 0.212191 kmol/h at 450 ^{O}C. The $FeSO_4$, was favored below 450 ^{O}C, where it decreases from 0.158821kmol/h at 300 ^{O}C up to 0.059679 kmol/h at 425 ^{O}C. The good regeneration can be observed at 450 ^{O}C this prevents Sulfate formation. This is the same as Georgiadis et al.2020 who stated that the regeneration of the loaded sorbent with air or a diluted air stream was investigated in a similar simulation set-up, but is now equipped with a fluidized bed instead of a packed bed. Such a Gibbs reactor was required to control the very exothermal oxidation reaction. Results showed that the optimal regeneration temperature was 500 ^{O}C, as a compromise between sulfate production and reactivity and activity of the sorbent, [24][22].

The results show also ZnO, figure (E), regeneration increased from 0.003809kmol/h at 300 ^{O}C to 0.214431 kmol/h at 400 ^{O}C and it was observed sulfate decrease from 0.158227kmol/h at 300^{O}C to 1.60E-06kmol/h at 400 ^{O}C, this little sulfate persist up to 650 ^{O}C. This is consistent with Alonso et al., 2000, who said that due to the stability of zinc sulfate, regeneration must be carried out at temperatures greater than 720 ^{O}C,

which likely leads to excessive thermal sintering. Because Above 650 ^{O}C, sulfidation reduces zinc oxide to metallic zinc, which is then largely lost through evaporation [31].

For MnO regeneration figure 6(D) increase from 1.45E-05Kmol/h at 300 ^{O}C to 0.213492 kmol/h at 525 ^{O}C and the $MnSO_4$ was observed from 0.160169kmol/h at 300 ^{O}C to 6.06E-05kmol/h at 525 ^{O}C, these little traces were persisted up to 800 ^{O}C and ones can set the temperature above 800 ^{O}C. This study was in range with song, 2000 who indicated that an oxidative regeneration, and thermo-balance studies show that manganese sulfate($MnSO_4$) formation becomes unstable above 800 ° while MnO is the stable phase in sulfidation in all range of temperatures and manganese sulfate is stable below 800 ^{O}C during the regeneration process and operating conditions for obtaining a good performance of a sorbent [32].

3.8.2. Effect of inlet Pressure

The figures below represent the regenerability of 5 metal oxide with pressure 1 to 20 atm

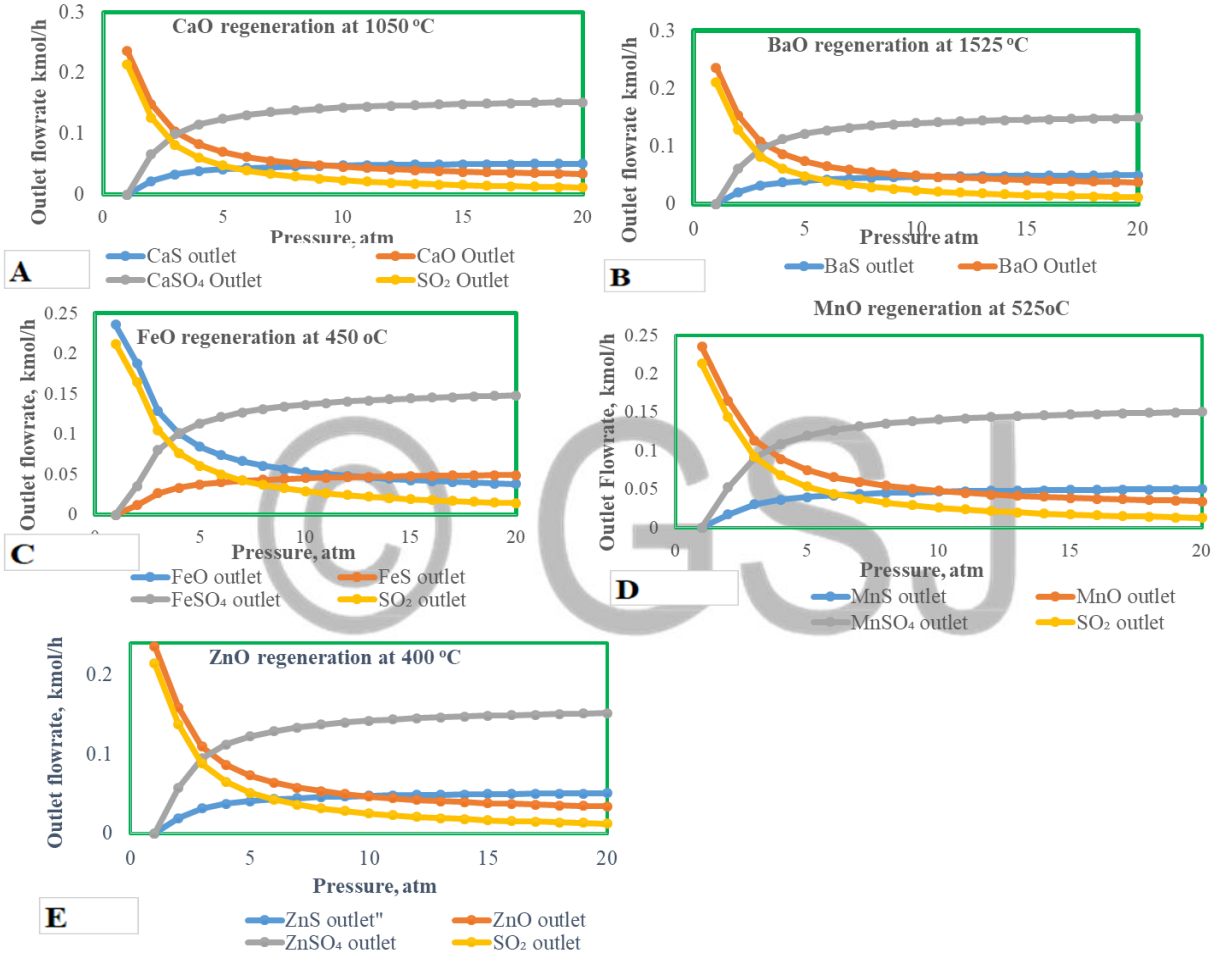

Figure 7. Effect of pressure on regeneration

The figure 7(A) above indicate that at 1050 ^{O}C mole flowrate CaO decreased from 0.2359kmol/h to 0.033656kmol/h when pressure increased from 1atm to 20atm respectively while $CaSO_4$ increased by 0 to 0.15167kmol/h, by maintaining temperature constant at 1525 ^{O}C, mole flowrate of BaO figure 7(B) decrease from 0.2359kmol/h to 0.03723kmol/h when increasing pressure from 1 to 20atm this favor the formation of $BaSO_4$ from 0 to 0.148994kmo/h.

Figure 7(C) also show at constant temperature of 450 ^{O}C, FeO decreased from 0.23588kmol/h to 0.038338kmol/h while $FeSO_4$ increase from 0 to 0.14816kmol/h when pressure increase from 1 to 20atm. The pressure impact also observed on MnO adsorbent Figure 7(D) at constant temperature of 525 ^{O}C, MnO molar flowrate decrease from 0.2351051kmol/h to 0.034588kmol/h when MnSO4 increased from 6X10-6kmol/h to 0.15044kmol/h, figure 14(E) also indicate at temperature of ZnO decrease from 0.235884kmol/h to 0.0339135kmol/h and $ZnSO_4$ 1.60x10^{-6}kmol/h to 0.151479kmol/h.

Generally, it is indicated that High pressure generally, doesn't favor the regeneration of metal oxide. This thermodynamic equilibrium analysis reveals that at the optimum temperature regenerating any metal oxide

by increasing pressure leads to the decreasing formation of metal oxide and sulfur dioxide on another hand it favors the sulfate formation. This emphasizes that operating at high pressure in regeneration during sulfurization is not recommended. The best operating pressure should be 1 atm. Because the pressure is reached, oxidation takes place quickly, accompanied by the generation of SO_2. Higher pressure favors sulfate production, while lower pressure ensures a high concentration of SO_2[33].

CONCLUSION AND RECOMMENDATION

The simulation of 5 metal oxides including CaO, BaO, FeO, MnO, and ZnO for H_2S removal in natural gas under influence of CO_2 was performed under their thermodynamic analysis. The feasibility was defined as H_2S removal efficiency of more than 98% and the existence of thermal stable components Thermodynamic calculations appeared to be a very useful tool to estimate gas phase and solid phase compositions during sulfiding and regeneration.

At low temperatures FeO and ZnO are the most performed while MnO was well performed at 200 ^oC and above due to the influence of CO_2 concentration. The alkali metal oxide such as CaO and BaO have been proven as the most performance at elevated temperatures, while at low temperatures showed a greater CO_2 removal. Changing CO_2 concentration in nature show an impact on BaO and CaO while has no significate effect on ZnO, MnO, and FeO due to the reactivity of metal oxide. Increasing pressure in the desulfurization process where the CO_2 is sensitive to the metal oxide such as alkali metal favor the CO_2 removal while H_2S removal efficiency is reduced and the Transition metals show no effect on increasing pressure.

Thermodynamic considerations show at medium temperatures, single oxides of Ca, Mn, Fe, or Ba won't achieve synthesis gas requirements but can be achieved in other application. Due to their specific temperature. 5 candidate solids based on the elements Fe, Zn, Mn, Ca, and Ba can be selected for Clean natural gas concentrations of <60ppb for H_2S. Based on the thermodynamic equilibrium

FeO, MnO, and znO are the most promising in the regeneration process at temperatures less than 800^oC, while BaO and CaO regenerate well at temperatures greater than 1050 ^oC.

For future works, it is recommended more detailed research on the effect of the adsorbent on other compounds in the natural gas feed has to be done. This is to avoid contamination of desulphurized gas after the process.

Further studies will be necessary to study the structural changes in the material and to determine regeneration conditions yielding SO_2 concentrations sufficiently high for H_2SO_4 production.

Nomenclatures

C_0	Initial concentration	(mg/l)
C	Equilibrium concentration	(mg/l)

ΔHr: enthalpy of reaction

ΔG……Gibbs free energy

Kp: Equilibrium constant

viations

RE Removal efficiency

ppmv**……** part per million volume

BTU.....British Thermal Unit

NG……...natural gas

Acknowledgment

The authors acknowledged the financial support from the World Bank funds under the Eastern & Southern Africa Higher Education Centers of Excellence (ACEII) Project, in which the Center of Studies in Oil and Gas Engineering and Technology (CS-OGET) of the Eduardo Mondlane University is a beneficiary

REFERENCE

[1] C. Frilund, P. Simell, N. Kaisalo, E. Kurkela, and M. L. Koskinen-Soivi, "Desulfurization of Biomass Syngas Using ZnO-Based Adsorbents: Long-Term Hydrogen Sulfide Breakthrough Experiments," *Energy and Fuels*, no. 5, 2020, doi: 10.1021/acs.energyfuels.9b04276.

[2] F. Danielsson, R. Fendler, M. Hailwood, and J. Shrives, "Analysis of H 2 S – incidents in geothermal and other industries," p. 52, 2009.

[3] A. Mohebbi, "CFD Simulation of a Wetted-Wall Column for Natural Gas Sweetening Using DEA Solution," vol. 5, no. 2, 2018.

[4] M. Rezakazemi, Z. Niazi, M. Mirfendereski, S. Shirazian, T. Mohammadi, and A. Pak, "CFD simulation of natural gas sweetening in a gas-liquid hollow-fiber membrane contactor," *Chem. Eng. J.*, vol. 168, no. 3, pp. 1217–1226, 2011, doi: 10.1016/j.cej.2011.02.019.

[5] N. Q. Long and T. X. Loc, "Experimental and modeling study on room-temperature removal of hydrogen sulfide using a low-cost extruded Fe2O3-based adsorbent," *Adsorption*, vol. 22, no. 3, pp. 397–408, 2016, doi: 10.1007/s10450-016-9790-0.

[6] G. T. Rochelle, "Amine Scrubbing for CO2 Capture," *Science (80-.).*, vol. 325, no. 5948, pp. 1652–1654, 2009, doi: 10.1126/science.1176731.

[7] L. Neveux *et al.*, "New insight into the ZnO sulfidation reaction : mechanism and kinetics modeling of the ZnS outward growth To cite this version : HAL Id : hal-00771115," 2013.

[8] C. Weinlaender, R. Neubauer, and C. Hochenauer, "Low-temperature H2S removal for solid oxide fuel cell application with metal oxide adsorbents," *Adsorpt. Sci. Technol.*, vol. 35, no. 1–2, pp. 120–136, 2017, doi: 10.1177/0263617416672664.

[9] M. Hedayat, M. Soltanieh, and S. A. Mousavi, "Simultaneous separation of H2S and CO2 from natural gas by hollow fiber membrane contactor using mixture of alkanolamines," *J. Memb. Sci.*, vol. 377, no. 1–2, pp. 191–197, 2011, doi: 10.1016/j.memsci.2011.04.051.

[10] F. J. Gutiérrez Ortiz, P. G. Aguilera, and P. Ollero, "Modeling and simulation of the adsorption of biogas hydrogen sulfide on treated sewage-sludge," *Chem. Eng. J.*, vol. 253, pp. 305–315, 2014, doi: 10.1016/j.cej.2014.04.114.

[11] R. K. Abdulrahman, I. M. Sebastine, and F. Z. Hanna, "Natural Gas Dehydration Process Simulation and Optimization : a Case study of Khurmala Field in Iraqi Kurdistan Region," *Int. J. Eng. Technol.*, vol. 4, no. 1, pp. 43–47, 2014.

[12] J. Alaei Kadijani and E. Narimani, "Simulation of hydrodesulfurization unit for natural gas condensate with high sulfur content," *Appl. Petrochemical Res.*, vol. 6, no. 1, pp. 25–34, 2016, doi: 10.1007/s13203-015-0107-0.

[13] M. P. González-Vázquez, F. Rubiera, C. Pevida, D. T. Pio, and L. A. C. Tarelho, "Thermodynamic analysis of biomass gasification using aspen plus: Comparison of stoichiometric and non-stoichiometric models," *Energies*, vol. 14, no. 1, 2021, doi: 10.3390/en14010189.

[14] A. Samokhvalov and B. J. Tatarchuk, "Characterization of active sites, determination of mechanisms of H 2S, COS and CS2 sorption and regeneration of ZnO low-temperature sorbents: Past, current and perspectives," *Phys. Chem. Chem. Phys.*, vol. 13, no. 8, pp. 3197–3209, 2011, doi: 10.1039/c0cp01227k.

[15] T. Pro, P. F. Diagrams, and O. L. E. Automation, "Reactor Calculation using Simulation Software," no. 1, pp. 1–16, 2001.

[16] M. S. E. R. K. T. B. M. Halvorsen, "Aspen Plus Simulation of Biomass Gasification with known Reaction Kinetic," pp. 149–156, 2015, doi: 10.3384/ecp15119149.

[17] S. H. Fogler, *Elements of Chemical Reaction Engineering, Printice- Hall International Editions*. 1987.

[18] M. Bülow, W. Lutz, and M. Suckow, "The mutual transformation of hydrogen sulphide and carbonyl sulphide and its role for gas desulphurization processes with zeolitic molecular sieve sorbents," *Stud. Surf. Sci. Catal.*, vol. 120 A, pp. 301–345, 1999, doi: 10.1016/s0167-2991(99)80556-4.

[19] C. Kunze and H. Spliethoff, "Modelling of an IGCC plant with carbon capture for 2020," *Fuel*

Process. Technol., vol. 91, no. 8, pp. 934–941, 2010, doi: 10.1016/j.fuproc.2010.02.017.

[20] Y. S. Hong, K. R. Sin, J. S. Pak, C. J. Kim, and B. S. Liu, "Kinetic Analysis of H2S Removal over Mesoporous Cu-Mn Mixed Oxide/SBA-15 and La-Mn Mixed Oxide/KIT-6 Sorbents during Hot Coal Gas Desulfurization Using the Deactivation Kinetics Model," *Energy and Fuels*, vol. 31, no. 9, pp. 9874–9880, 2017, doi: 10.1021/acs.energyfuels.7b00048.

[21] J. C. Lavalley, "Infrared spectrometric studies of the surface basicity of metal oxides and zeolites using adsorbed probe molecules," *Catal. Today*, vol. 27, no. 3–4, pp. 377–401, 1996, doi: 10.1016/0920-5861(95)00161-1.

[22] A. G. Georgiadis, N. Charisiou, I. V. Yentekakis, and M. A. Goula, "Hydrogen sulfide (H2S) Removal via MOFs," *Materials (Basel).*, vol. 13, no. 16, 2020, doi: 10.3390/MA13163640.

[23] D. P. Harrison, "Performance Analysis of ZnO-Based Sorbents in Removal of H2S From Fuel Gas," *Desulfurization Hot Coal Gas*, no. 1, pp. 213–242, 1998, doi: 10.1007/978-3-642-58977-5_11.

[24] D. M. Wang, "Breakthrough Behavior of H2S Removal with an Iron Oxide Based CG-4 Adsorbent in a Fixed-Bed Reactor," no. September, p. 136, 2008.

[25] J. A. B. Obek, D. Ó. R. A. R. I. E. T. H. Ő, É. V. A. M. Olnár, and R. Ó. B. Ocsi, "SELECTIVE HYDROGEN SULPHIDE REMOVAL FROM ACID GAS BY ALKALI CHEMISORPTION IN A JET REACTOR," vol. 44, no. 1, pp. 51–54, 2016, doi: 10.1515/hjic-2016-0006.

[26] Y. Hongyun, R. Sothen, D. R. Cahela, and B. J. Tatarchukt, "Breakthrough characteristics of reformate desulfurization using zno sorbents for logistic fuel cell power systems," *Ind. Eng. Chem. Res.*, vol. 47, no. 24, pp. 10064–10070, 2008, doi: 10.1021/ie8008617.

[27] I. I. Novochinskii *et al.*, "Low-temperature H2S removal from steam-containing gas mixtures with ZnO for fuel cell application. 1. ZnO particles and extrudates," *Energy and Fuels*, vol. 18, no. 2, pp. 576–583, 2004, doi: 10.1021/ef030137l.

[28] V. Jalan, "Studies involving high temperature desulfurization regeneration reactions of metal oxides for fuel cell development Final report," *US DOE Rep. DOE/MC/16021-1486(DE84 003096)*, p. 130, 1983.

[29] B. Zeng, H. Li, T. Huang, C. Liu, H. Yue, and B. Liang, "Kinetic study on the sulfidation and regeneration of manganese-based regenerable sorbent for high temperature H2S removal," *Ind. Eng. Chem. Res.*, vol. 54, no. 4, pp. 1179–1188, 2015, doi: 10.1021/ie503233a.

[30] M. Flytzani-Stephanopoulos and Z. Li, "Kinetics of Sulfidation Reactions Between H_2S and Bulk Oxide Sorbents," *NATO ASI Ser.*, vol. G 42, pp. 179–211, 1998.

[31] L. Alonso and J. M. Palacios, "Performance and recovering of a Zn-doped manganese oxide as a regenerable sorbent for hot coal gas desulfurization," *Energy and Fuels*, vol. 16, no. 6, pp. 1550–1556, 2002, doi: 10.1021/ef020106a.

[32] Y. K. Song, K. B. Lee, H. S. Lee, and Y. W. Rhee, "Reactivity of Copper Oxide-Based Sorbent in Coal Gas Desulfurization," *Korean J. Chem. Eng.*, vol. 17, no. 6, pp. 691–695, 2000, doi: 10.1007/BF02699119.

[33] A. Palmer, P. Heeney, and E. Furimsky, "R e g e n e r a t i o n of Iron Oxide Containing Pellets Used for Hot Gas Clean Up," vol. 23, pp. 75–85, 1989.